University of Baghdad
College of Engineering
JOURNAL OF ENGINEERING

Journal of Engineering

journal homepage: www.jcoeng.edu.iq

Volume 31 Number 7 July 2025

Comparison of the Hydraulic Effect of Straight and Curved Groynes in the Curved Canal

Yousif. Z. Salim *, **Hayder A. K. Al-Thamiry**

Department of Water Resources Engineering, College of Engineering, University of Baghdad, Baghdad, Iraq

ABSTRACT

The dynamics of flow and turbulence surrounding groynes in a bending canal are highly complex behaviors. This study, which was conducted by HEC-RAS version 6.5 software, focuses on the use of curved groynes in 180°-degree bend canals to study the flow behavior in bending by calculating the velocity of flow along the concave outer edge, in which bank erosion usually occurs, the flow velocity at the inner edge, and calculating the vortices that form between the groynes. The results showed that the curved groynes outperformed the commonly used straight groynes in the same conditions. The findings indicate that curved groins decrease the flow velocity at the outer edge by 99%, while straight groins achieve a reduction in flow velocity ranging from 68% to 98%. Due to the decrease in the canal section, the increase in flow velocity at the inner edge was 28% for curved groynes and 34% for straight groynes. Additionally, curved groynes reduce the vortex value within the groynes field, thereby reducing the scouring rate in the canal bed.

Keywords: Groynes, Curved groynes, Straight groynes, Curved canals, HEC-RAS.

1. INTRODUCTION

Natural rivers and water bodies form their bottoms from mobile particles like gravel, sand, and silt, not from permanent ones. Sediment transport is the mechanism by which water flow moves and changes sediments. The river transports these sediments to various reservoirs, altering the river's course, diminishing the reservoir's capacity, and lowering the navigable depth. As a result, the river bends. Ditches and similar structures were used to protect the banks of the river bend on the concave sides of the canals. The pattern of erosion deposition in meander rivers leads to channel migration, negatively affecting river management and agricultural production. Various forms of river training structures, such as bend way weirs, rock vanes, stream barbs, and bank-attached vanes, are currently undergoing testing **(Azizipour et al., 2020; Siefken et al., 2021).** Dikes and groynes are made to waterways as additional engineering construction for controlling bank erodibility, sedimentation, regulating water level, shifting the river flow for enhanced navigation, and

*Corresponding author
Peer review under the responsibility of University of Baghdad.
https://doi.org/10.31026/j.eng.2025.07.04

Article received: 24/01/2025
Article revised: 23/03/2025
Article accepted: 13/04/2025
Article published: 01/07/2025

so forth. They are termed as coastal protection works, which are usually placed at right angles to the shore for the purpose of preventing coastal or beach erosion. They are positioned on the front side of the bank to serve as protection against erosion of the bank and levee **(Uijttewaal, 2005)**. Apart from the construction features aimed at maintaining depth of the channel and protecting the river bank, the groynes on rivers also significantly improve the local biological basin of the river and increase the volume of the water that can be occupied by living organisms **(Ohmoto et al., 2002; Deng et al., 2019)**.

Such structures are now prevalent in river and coastal engineering, incurring recent studies like laboratory investigations conducted by **(Ettema and Muste, 2004)** and their previous computational and analytical investigations. Directly downstream of the spur-dike, the study revealed the extent of the catchment area and the alignment of the flow-thalweg surrounding it. **(Kadota and Suzuki, 2010**) investigated mean and coherent flow structures during visual inspection of the flow patterns surrounding T and L groins. Researchers have extensively studied scour around abutments, **(Kothyari and Ranga Raju, 2001)** used an analogous pier model to calculate the temporal fluctuation of scour around spur-dikes and bridge abutments. **(Dey and Barbhuiya, 2006)** examined 3D turbulent flow in a scour hole at a vertical-wall abutment under clear water conditions, revealing a dominant upstream vortex and chaotic downstream flow, providing essential data for improving scour prediction models. **(Barbhuiya and Dey, 2003)** examined the various abutment studies and gave a thorough analysis of the flow field, abutment scour, the time variation of scour depth, and the formulas for estimating scour depth. **(Dey and Barbhuiya, 2005)** studied the scouring at abutments throughout time. The maximum scour depth for a sand-gravel mixture occurs at the sand bed's upstream tip. However, researchers have not studied the processes and flow behavior around groins and gravel beds. **(Kuhnle et al., 2008)** examined flow and scour around submerged trapezoidal spur dikes using lab measurements and CCHE3D simulations. Detailed velocity data revealed distinct near-field flow patterns compared to non-submerged cases. The model accurately captured flow fields but showed minor discrepancies in bed shear predictions. Findings enhance understanding of spur dikes' impact on sediment transport and erosion, though local scour modeling still requires refinement.

(Gu et al., 2020) identified velocity similarity near dike tips as the main factor controlling spacing thresholds of non-submerged twin spur dikes, with minimal influence from Froude number and a convex quadratic relationship with B/b and B/h. **(Shampa et al., 2020)** claimed that the high-permeability spur-dike group may improve transverse flow while lowering the channel's longitudinal turbulence intensity and velocity. **(Masjedi et al., 2010)** conducted a thorough analysis of how wing design influences the reduction of local scour at a T-shaped spur dike in a 180° laboratory experimental flume bend. At the bend, tests were carried out for three different wing shapes of T-shaped spur dikes with different Froude numbers. **(Akbari et al., 2021)** compared variations in the mean flow pattern along a 180° bend with various T-shaped spur dike lengths. The findings indicate that positioning the spur dike at the bend apex increases mean secondary flow strength by 2.5 times, and a 67% increase in the wing and web length leads to a 27% growth in mean secondary flow strength along the bend. **(Ghodsian and Vaghefi, 2009)** presented a T-shaped spur dike in a 90°channel bend through an experimental finding on the flow field and scour surrounding. Experiments indicated that while scour increased with increasing the length of the spur dike and Froude number, it decreased with an increase in the wing length of the spur dike. The vortices of larger diameters occurred due to increasing upstream scouring and an expanded flow separation zone**. (Sharma and Mohapatra, 2012)** explained in a laboratory

experimental study on flow past a spur dyke on a fixed bed meandering channel found that downstream separation zone length varies based on the spur dyke's position, and at higher elevations, it is wider. The study furthermore analyzed the contraction ratio and inflow Froude number effects. **(Vaghefi et al., 2017)** conducted an experimental study using a 3-D acoustic Doppler velocimeter to investigate the flow field around a T-shaped spur dike that was in a 90° bend experimental canal. According to the data, secondary flow patterns showing horizontal vortices in both upstream and downstream directions were greatly affected by the spur dike. Variations in vorticity and secondary flow were also examined. **(Mehraein et al., 2014)** analyzed the impact of the spur dike placing on the flow field a 90°-degree sharp bend canal including spur dike, three distinct points along a bend were used for velocity measurements. According to the results, the flow field changes a lot. For example, at θ = 60°, the bed shear stress and sweep and ejection event probability are the lowest.

By focusing on the study local scour around groynes (elliptic and semi-parabolic) shapes in straight experimental canal under variable conditions, using the MATLAB program and dimensional analysis to calculate the maximum scour depth, elliptic groins reduce the scour depth and the volume of deposition by a lower percentage than when using the second form by comparing the results **(Ibrahim and AL-Thamiry, 2018)**.

(Majeed et al., 2022; AL-Sarefi and Azzubaidi, 2021) used (CFD) software to study the impact of (parabolic and elliptical) groynes number on maximum cleaning depth and bed shear stress in a straight canal. **(Kirti, 2018)** analyzed the placement of straight groynes in river bends with 20 m width to protect the banks from corrosion using CFD software. The results showed that the best location of the groynes is the first quarter of the bend at an angle of 15 degrees; it reduces corrosion and improves water flow. The groins with a length of 3.5 meters and a width of 0.5 meters were the most efficient in achieving these goals, this confirms the importance of careful planning of the location and angle of groynes installation. However, HEC-RAS software is one of the most important programs used to analyze the behavior of flow velocity in rivers, reservoirs, hydraulic characteristics, and sediment transport. To analyze sediment transport and water flow in Iraqi canals and rivers, the HEC-RAS software was used in many studies that focused on morphological changes, erosion, sedimentation phenomena, and their impact on the efficiency of water transport systems. HEC-RAS software proved its efficiency through accurate simulation models, which helped in the development of rivers and the management of water resources **(Nama, 2011; Daham and Abed, 2020; Jassam and Abed, 2021; Daher and Ameen, 2024; Razzaq et al., 2024). (Altawash and Al Thamiry, 2022; Al-dahhan and Al-Juhaishi, 2024)** studied the hydraulic characteristics of dam reservoirs using the correspondence rate between the HEC-RAS software results and field measurements. This rate was more than 99 percent.

HEC-RAS was used to calibrate Manning's coefficient in the Euphrates River between Haditha Dam and Ramadi Barrage, achieving highly accurate simulation results with minimal error (RMSE = 0.267) based on extensive cross-sectional and multi-year discharge data **(Hashim and Azzubaidi, 2023)**.

This study aims to investigate flow velocity patterns at both edges and vortex formation between groynes in a 180° bend canal with curved groynes, and to compare their effectiveness with straight groynes

2. JUSTIFICATION OF THE RESEARCH

The bank of the meander open channel is influenced by some factors for stability, including the hydraulic structures present in the rivers, such as their shape and the percentage of blockages within the river, as well as flow characteristics, such as flow discharge and depth,

and soil characteristics, such as particle size, uniformity, and consistency. This study will only discuss the effect of curved groynes in meandering rivers because few studies have examined how they affect flow velocity at both boundaries of the bend zone.

3. VALIDATION OF THE HEC-RAS SOFTWARE MODEL IN THE CURVED CANAL

Based on laboratory experiment data **(Leschziner and Rodi, 1979)**, the HEC-RAS program assesses flow velocity in a curved canal, as no experiments have evaluated flow velocity in a curved canal with groynes. The HEC-RAS 2D software used data from the laboratory canal to create a 180° topography of the curved canal, incorporating modifications to improve our understanding of the flow behavior within the canal. **Fig. 1** represents velocity profile lines across the experiment canal and HEC-RAS model at the locations (A-A) and (B-B) that will be compared. **Fig. 2 (A and B)** showed the velocity results from the HEC-RAS software and the measured velocities experimental data **(Leschziner and Rodi, 1979; Molls and Chaudhry, 1995)**

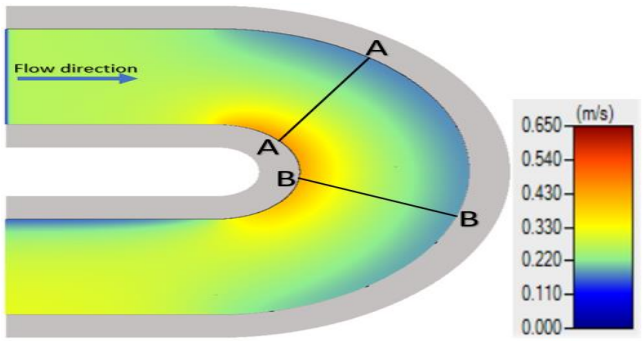

Figure 1. Flow velocity distribution value for sections (A-A) and (B-B).

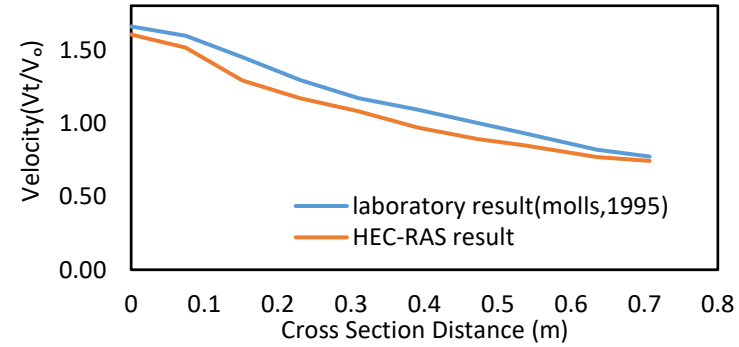

(A)

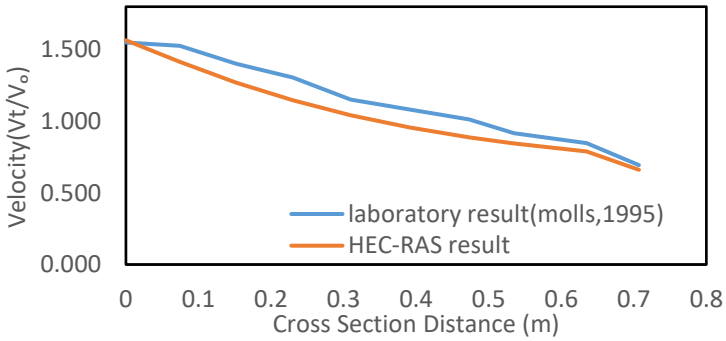

(B)

Figure 2. (A)Velocity distribution for cross section (A-A) (B) Velocity distribution for cross section (B-B).

4. IMPLEMENTATION OF THE MODEL

The bank of the meander open channel is influenced by some factors for stability, including the hydraulic structures present in the rivers, such as their shape and the percentage of blockages within the river, as well as flow characteristics, such as flow discharge and depth, and soil characteristics, such as particle size, uniformity, and consistency. The effect of curved groynes in meandering rivers will only be covered in this section because there are few studies on these elements and the extent to which they affect the flow velocity at both edges of the bend zone in river bends.

4.1 Effect of Groyne Shape on Flow Behavior

Groyne dimensions were determined based on validated hydraulic design principles and prior studies. The length was set to one-fourth of the channel width, a ratio shown to redirect flow effectively while minimizing turbulence and sediment disturbance **(Akbari et al., 2021; AL-Sarefi and Azzubaidi, 2021)**. Spacing between groynes was set at 2.5 times the projection length (W), a standard in optimizing flow and sediment control. Orientation angles were selected for their proven efficiency in reducing bank erosion and enhancing flow stability **(Kirti, 2018)**. These geometric parameters for both straight and curved groynes are illustrated in **Fig. 3(A and B)**

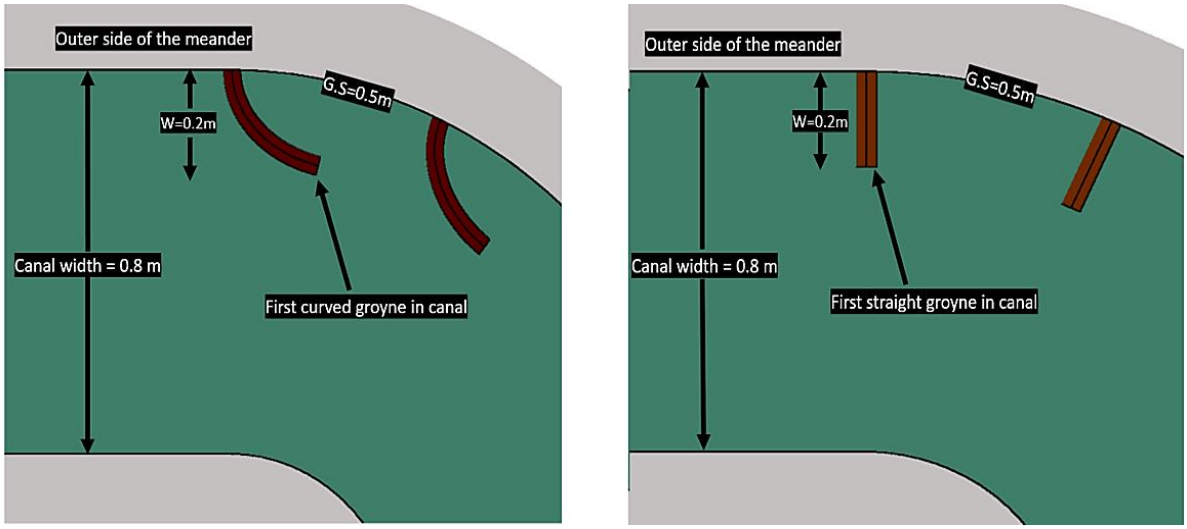

(A) **(B)**

Figure 3. (A) Curved groynes properties in canal. (B) Straight groynes properties in canal.

4.2 Model Mesh

HEC-RAS software has a meshing-generating software. Independent meshes compose each component of the model. The tetrahedron assembly meshing approach works well for the relevant center; height was chosen for high-quality smoothing, and proximity and curvature were chosen for improving size function. Until every configuration reaches the optimal meshing quality, the process continues. To create the two-dimensional flow regions, draw a polygon line in the geometry window. Next, create the grid by entering the number for the gap between each grid. A mesh cell size of 0.02 m was chosen for all channels to determine the distance between each grid, as shown in **Fig. 4**.

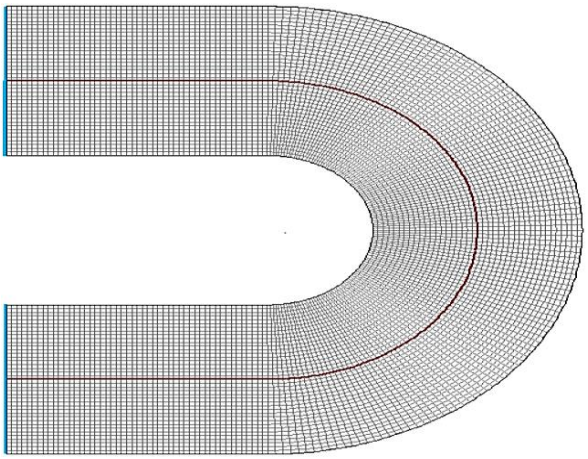

Figure 4. Mesh spacing size for 180° bend test case.

4.3 Boundary Conditions

It is important to clarify that this study did not involve new laboratory experiments. Instead, previously published experimental data **(Leschziner and Rodi, 1979; Molls and Chaudhry, 1995)** were used for model calibration and validation. The baseline case for validation was a natural flow condition without groynes, ensuring that the numerical model accurately replicated real hydraulic conditions. After calibration, the model was extended to analyze the effects of groynes on flow dynamics in a curved canal by introducing groyne structures for comparison. The boundary conditions, including a discharge of 0.0123 m^3/s and a water height of 0.057 m, were adopted directly from the experimental data provided by **(Leschziner and Rodi, 1979; Molls and Chaudhry, 1995)** to validate the HEC-RAS 6.5 model. As no additional laboratory experiments were conducted in this study, these parameters ensured consistency with established experimental constraints for accurately simulating flow behavior in a 180°bend canal.

4.4 Mathematical Equations

The hydrodynamic behavior of flow in the curved canal with groynes is governed by the Shallow Water Equations (SWE), which describe mass and momentum conservation for incompressible, free-surface flow and are expressed as follows:
Continuity Equation (Mass Conservation):

$$\frac{\partial h}{\partial t} + \frac{(\partial hu)}{\partial x} + \frac{(\partial hv)}{\partial y} = 0 \quad (1)$$

Where:
h is the water depth. The u and v are velocities in the x and y directions, t is the time (s)

Momentum Equations (Conservation of Momentum):
In the x-direction

$$\frac{(\partial hu)}{\partial t} + \frac{\partial}{\partial x}(h^2u^2 + \frac{1}{2}gh) + \frac{\partial(huv)}{\partial x} = - gh\frac{\partial z}{\partial x} + fx \quad (2)$$

In the y-direction

$$\frac{(\partial hv)}{\partial t} + \frac{\partial}{\partial x}(h^2v^2 + \frac{1}{2}gh) + \frac{\partial(huv)}{\partial y} = - gh\frac{\partial z}{\partial y} + fy \quad (3)$$

Where: g is gravitational acceleration, z represents the bed elevation, and fx , fy denote frictional forces in their respective directions.

Centrifugal Force Effect on Pressure Distribution

$$\frac{V^2}{r}\rho = \frac{\partial P}{\partial r} \tag{4}$$

Where: P is pressure, ρ is water density, V is velocity
These equations underpin the evaluation of velocity distribution, turbulence characteristics, and flow separation in the 180° bend canal with groynes.

5. RESULTS AND DISCUSSION

The most important reliable results for comparing the types of groynes used in this research are the flow velocity between two consecutive groynes along the outer edge of the river and the amount of flow velocity obtained when using each shape separately. **Fig. 5** shows that the vortex velocity between the straight groynes at an angle of 90° increases the velocity of the vortices formed downstream of the third groyne, which is consistent with previous research **(Indulekha et al., 2021)**. On the other hand, **Fig. 6** presents the vortex velocity between the curved groynes, revealing a different flow behavior and intensity. The results indicate that the straight groyne generates a higher vortex velocity than the curved groyne, suggesting that the lowest vortex velocities occur when using curved groynes. This difference between **Figs. 5 and 6** highlights the reduction in flow turbulence when using curved groynes compared to straight ones. The color scale shown on the right side of **Figs. 5 and 6** represents the velocity magnitude in meters per second (m/s).

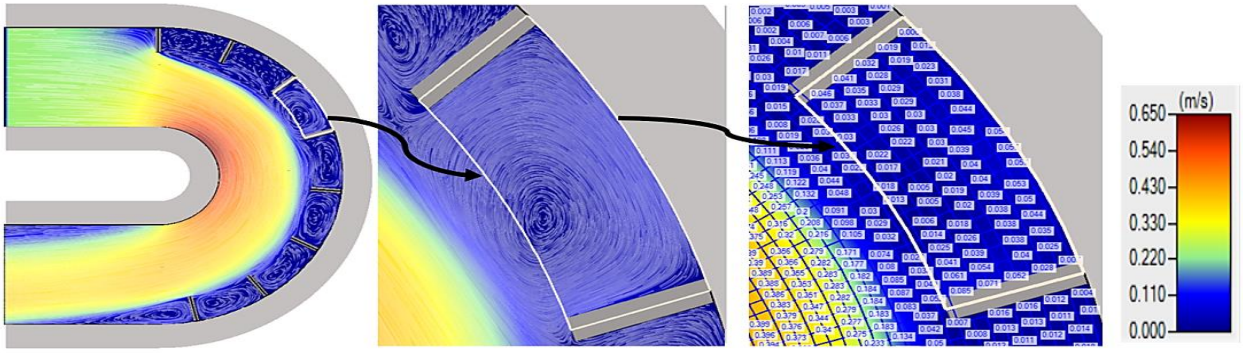

Figure 5. Vortices velocity value between groynes in bend 180° with straight groyne.

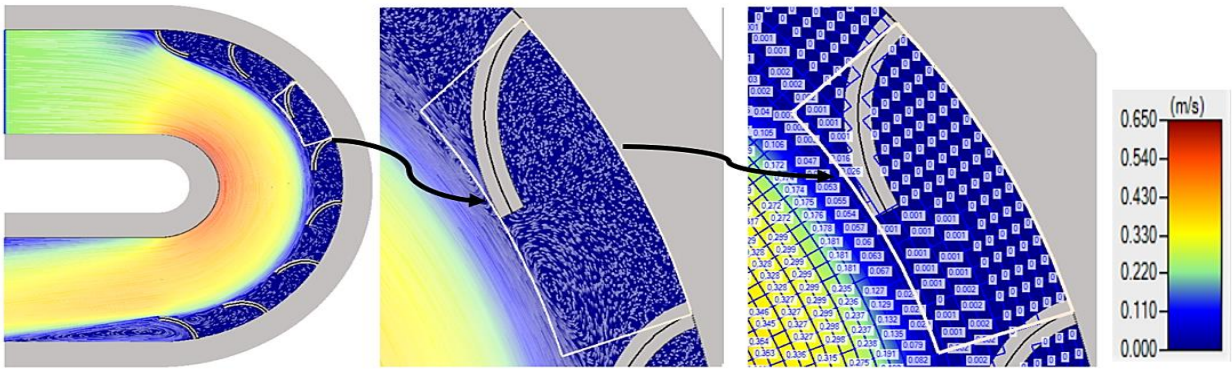

Figure 6. Vortices velocity value between groynes in 180° bend with curved groyne.

These findings confirm that curved groynes significantly improve hydraulic efficiency by reducing turbulence and stabilizing flow conditions in curved channels. Their impact on reducing local scour and maintaining channel stability makes them a more effective alternative to traditional straight groynes.

The HEC-RAS software's simulations showed that the calculated flow velocity values were very different along the outer edge of the meander zone and in the area close to the inner edge of the canal. This is because there are different types of groynes in those areas. **Fig. 7** illustrates this variation, highlighting low-velocity areas in blue and high-velocity areas in red.

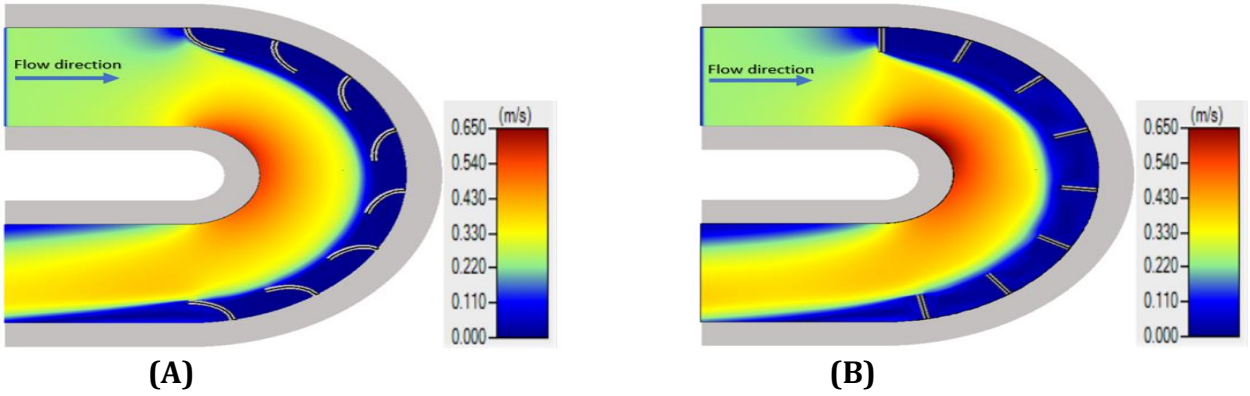

(A) **(B)**

Figure 7. Velocity distribution along canal 180°bend (A) curved groyne (B) straight groyne.

Fig. 8 displays the calculated flow velocity for each of the three cases: one case without groynes and two cases before and after the addition of different types of groynes. The figure highlights the effects of groynes on velocity distribution, particularly emphasizing how straight groynes create substantial velocity fluctuations along the outer edge due to vortex shedding and turbulent flow interactions. The alternating acceleration and deceleration regions observed in the velocity profile indicate unstable flow patterns, which contribute to increased turbulence and sediment transport. This fluctuation is most evident downstream of the third groyne where continuous interactions between vortices and the main flow intensify velocity variations while curved groynes reduce these fluctuations by altering the flow structure through their streamlined shape which limits abrupt separations and weakens vortex strength allowing smoother transitions and a more uniform velocity field as shown in **Fig. 8** where regions influenced by curved groynes display lower turbulence intensity and reduced sediment transport.

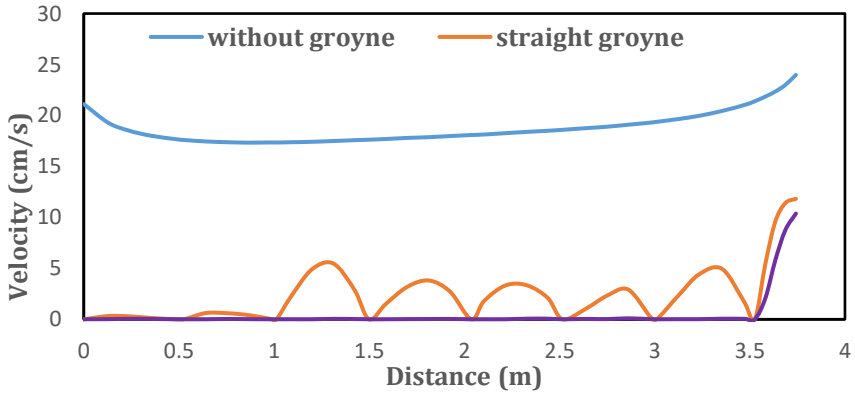

Figure 8. Velocity distribution along the outer edge of bend 180°.

As illustrated in **Fig. 9** the velocity distribution along the inner bank highlights an acceleration caused by flow contraction due to groyne presence that redirects the main current inward increasing velocity near the inner edge and showing that straight groynes generate sharper velocity peaks due to their angular geometry which promotes stronger flow separation and secondary circulation whereas curved groynes guide the flow more gradually reducing velocity gradients and contributing to a more stable hydrodynamic environment which influences sediment transport by minimizing erosion and channel bed deformation and ultimately decreasing the risk of sediment displacement

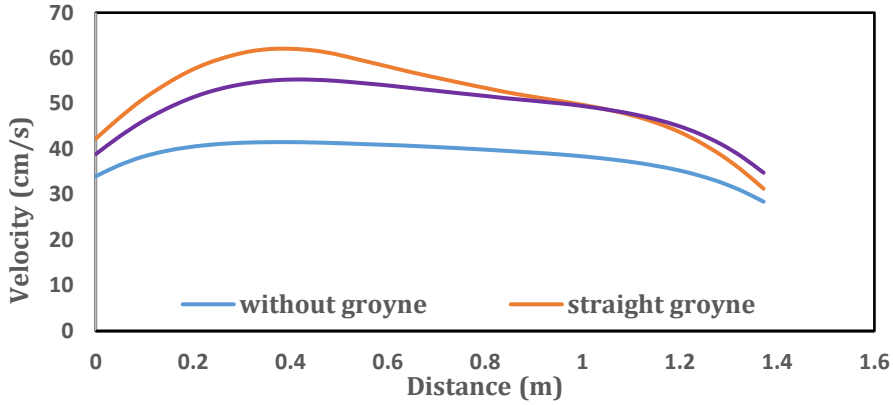

Figure 9. Velocity distribution along the inner edge of 180°bend.

Table 1 displays the summaries of maximum flow velocity values along the outer edge of the canal bend for each distance between consecutive groynes, regardless of whether they are straight, curved, or absent. **Table 2** displays the summaries of maximum velocity values at the inner edge of the bend canal in all scenarios, including the presence and absence of groynes in their various forms, and illustrates the impact of groynes on the flow velocity in this area.

Table 1. Max velocity along the outer edge of the bend between two consecutive groynes.

Distance (m)	Without groyne (cm/s)	Straight groyne (cm/s)	Curved groyne (cm/s)	Velocity reduction ratio straight groyne %	Velocity reduction ratio curved groyne %
0 - 0.5	21.1	0.34	0.042	98.39	99.80
0.5 - 1	17.6	0.65	0.03	96.31	99.83
1 - 1.5	17.63	5.57	0.04	68.41	99.77
1.5 - 2	18.07	3.81	0.03	78.92	99.83
2 - 2.5	18.59	3.45	0.084	81.44	99.55
2.5 - 3	19.41	3	0.1	84.54	99.48
3 - 3.5	21.01	5.05	0.07	76	99.67

Table 2. Maximum velocity along the inner edge of the bend.

Distance (m)	Without groyne (cm/s)	Straight groyne (cm/s)	Curved groyne (cm/s)	Velocity increase ratio straight groyne %	Velocity increase ratio curved groyne %
0	34.03	42.3	38.9	24.30	14.31
0.5	41.28	60.62	54.91	46.85	33.02
1	38.30	49.55	49.33	29.37	28.80
1.38	28.44	31.3	34.80	10.06	22.36

6. CONCLUSIONS

The study showed that using curved groynes instead of the more common straight groynes changed the flow behavior at the concave edge of the bending zone in a big way. The vortices between the curved groynes also behaved better. The following are the main conclusions.

1. When using curved groynes at the outer edges of the canal, the flow velocity value is at its lowest, greatly enhancing the stability of the banks and preventing their erosion due to high velocity.
2. Using curved groynes to narrow the canal section results in a lower rate of flow velocity rise at the inner edge of the canal compared to using straight groynes. This is beneficial for protecting the inner side of the canal because it stops the flow velocity from rising too quickly.
3. Curved groynes provide greater protection to the bottom of the canals by reducing the vortices and protecting the bed from scour.

To further enhance the understanding and effectiveness of curved groynes in curved canals, future research should focus on optimizing their design parameters, including curvature angle, spacing, and orientation, to achieve the best balance between flow regulation and erosion control. Additionally, investigating the long-term performance of curved groynes under different hydraulic and environmental conditions is crucial to ensure their durability and efficiency. Further experimental validation through large-scale laboratory tests and field applications in real-world river systems will help refine numerical models and improve practical implementations. Moreover, assessing their impact on sediment transport and deposition patterns can aid in preventing unwanted accumulation and maintaining channel stability over time.

NOMENCLATURE

Symbol	Description	Symbol	Description
v_o	Entrance velocity m/s	h	Water depth m
v_t	Velocity profile m/s	g	Gravitational acceleration m/s^2
%	percentage	z	Bed elevationm
m	Station m	*fx , fy*	Frictional forces in x and y directions N
Q	Discharge (m^3/s)	P	Pressure Pa
V	Velocity (cm/s)	ρ	Water density kg/m^3

Acknowledgments

This work was supported by the (water resource engineering department, University of Baghdad).

Credit Authorship Contribution Statement

Yousif Zaid and Hayder. A. K. Al-Thamiry: Writing – review & editing, Writing – original draft, Validation, Methodology.

Declaration of Competing Interest

The authors confirm that they do not have any competing financial interests or personal relationships that could have influenced the work reported in this paper.

REFERENCE

Akbari, M., Vaghefi, M. and Chiew, Y.-M., 2021. Effect of T-shaped spur dike length on mean flow characteristics along a 180-degree sharp bend. *Journal of Hydrology and Hydromechanics*, 69(1), pp. 98–107 http://dx.doi.org/10.2478/johh-2020-0045

AL-Sarefi, A.M.H. and Azzubaidi, R.Z., 2021. Investigations on the impact of using elliptic groynes on the flow in open channels. *Journal of Engineering*, 27(2), pp. 44–58. https://doi.org/10.31026/j.eng.2021.02.04

AL-dahhan, M. N. and Rashid Al-Juhaishi, M., 2024. Hydrodynamic evaluation of hemrin dam reservoir: morphological examination. *IOP Conference Series: Earth and Environmental Science,* 1374(1), P. 012066. https://doi.org/10.1088/1755-1315/1374/1/012066

Altawash, M.M. and Al Thamiry, H.A., 2022. Velocity patterns inside the proposed Makhool Dam Reservoir with different operation plans. *IOP Conference Series: Earth and Environmental Science*, 1120(1), P. 012015. https://doi.org/10.1088/1755-1315/1120/1/012015

Azizipour, M., Meymani, F.A. and Shooshtari, M.M., 2020. Enhancing scour protection in river bends: a novel slotted bank-attached vane. *Water Supply*, 20(6), pp. 2175–2184. https://doi.org/10.2166/ws.2020.116

Barbhuiya, A.K. and Dey, S., 2003. Vortex flow field in a scour hole around abutments. *International Journal of Sediment Research*, 18(4), pp. 310–325

Daham, M.H. and Abed, B.Sh., 2020. Simulation of sediment transport in the upper reach of Al-Gharraf River. *IOP Conference Series: Materials Science and Engineering*, 901(1), P. 012012. https://doi.org/10.1088/1757-899X/901/1/012012

Daher, A. R., and Ameen, M. S. (2024). Simulation of flow characteristics in open channels with inflatable dam. *IOP Conference Series: Earth and Environmental Science, 1374*(1), 012059. https://doi.org/10.1088/1755-1315/1374/1/012059

Deng, Y., Cao, M., Ma, A., Hu, Y. and Chang, L., 2019. Mechanism study on the impacts of hydraulic alteration on fish habitat induced by spur dikes in a tidal reach. *Ecological Engineering*, 134, pp. 78–92. http://dx.doi.org/10.1016/j.ecoleng.2019.05.003

Dey, S. and Barbhuiya, A.K., 2005. Time variation of scour at abutments. *Journal of Hydraulic Engineering*, 131(1), pp. 11–23. https://doi.org/10.1061/(ASCE)0733-9429(2005)131:1(11)

Dey, S. and Barbhuiya, A.K., 2006. Velocity and turbulence in a scour hole at a vertical-wall abutment. *Flow Measurement and Instrumentation*, 17(1), pp. 13–21. http://dx.doi.org/10.1016/j.flowmeasinst.2005.08.005

Ettema, R. and Muste, M., 2004. Scale effects in flume experiments on flow around a spur dike in flatbed channel. *Journal of Hydraulic Engineering*, 130(7), pp. 635–646. http://dx.doi.org/10.1061/(ASCE)0733-9429(2004)130:7(635)

Ghodsian, M. and Vaghefi, M., 2009. Experimental study on scour and flow field in a scour hole around a T-shape spur dike in a 90 bend. *International Journal of Sediment Research*, 24(2), pp. 145–158. https://doi.org/10.1016/S1001-6279(09)60022-6

Gu, Z., Cao, X., Gu, Q. and Lu, W.-Z., 2020. Exploring proper spacing threshold of non-submerged spur dikes with ipsilateral layout. Water, 12(1), P. 172. https://doi.org/10.3390/w12010172

Hashim, L.I. and Azzubaidi, R. Z., 2023. Roughness coefficient in Euphrates River Reach between Haditha Dam to Ramadi Barrage. *Journal of Engineering*, 29(3), pp. 117–124. https://doi.org/10.31026/j.eng.2023.03.08

Ibrahim, A.K. and AL-Thamiry, H.A., 2018. Experimental study of local scour around elliptic and semi-parabolic groynes in straight channels. *Association of Arab Universities Journal of Engineering Sciences*, 25(4), pp. 105–116

Indulekha, K.P., Jayasree, P.K. and Sachin, S., 2021. Simulation of flow pattern around series of groynes with different orientations in meandering channels. *IOP Conference Series: Materials Science and Engineering*, 1114(1), P. 012024. https://doi.org/10.1088/1757-899X/1114/1/012024

Jassam, W.A. and Abed, B.Sh., 2021. Assessing of the morphology and sediment transport of Diyala River. *Journal of Engineering*, 27(11), pp. 47–63. https://doi.org/10.31026/j.eng.2021.11.04

Kadota, A. and Suzuki, K., 2010. Local scour and development of sand wave around T-type and L-type groynes. In: Scour and Erosion. pp. 707–714.

Kirti, S., 2018. Study of effect of placement of groyne on sharp bend in river using CFD analysis. International Journal of Advanced Research, 6(3), pp. 153-161. http://dx.doi.org/10.21474/IJAR01/6661

Kothyari, U. and Ranga Raju, K., 2001. Scour around spur dikes and bridge abutments. *Journal of hydraulic research*, 39(4), pp. 367–374. http://dx.doi.org/10.1080/00221680109499841

Kuhnle, R.A., Jia, Y. and Alonso, C.V., 2008. Measured and simulated flow near a submerged spur dike. *Journal of Hydraulic Engineering*, 134(7), pp. 916–924. http://dx.doi.org/10.1061/(ASCE)0733-9429(2008)134:7(916)

Leschziner, M.A. and Rodi, W., 1979. Calculation of strongly curved open channel flow. *Journal of the Hydraulics Division*, 105(10), pp. 1297–1314. https://doi.org/10.1061/JYCEAJ.0005286

Majeed, H.Q., Abed, B.S. and Ibrahim, A.K., 2022. Countermeasure of riverbanks local scour and deposition using different shapes of multiple groynes with different spacing. *Mathematical Modelling of Engineering Problems*, 9(5), pp. 1277–1281. http://dx.doi.org/10.18280/mmep.090515

Masjedi, A., M.S. Bejestan and Rahnavard, P., 2010. Experimental Study on the Time Development of Local Scour on Around Single T-Shape Spur Dike in a 180 Degree Flume Bend. *Research Journal of Environmental Sciences*, 4, pp. 530-539. https://doi.org/10.3923/rjes.2010.530.539

Mehraein, M., Ghodsian, M. and Najibi, S., 2014. Experimental investigation on the flow field around a spur dike in a 90 sharp bend. Proc., 7th Int. Conf. on Fluvial Hydraulics, Taylor & Francis Group, Lausanne, Switzerland. pp. 743–749. http://dx.doi.org/10.1201/b17133-101

Molls, T. and Chaudhry, M.H., 1995. Depth-averaged open-channel flow model. Journal of Hydraulic Engineering, 121(6), pp. 453–465. https://doi.org/10.1061/(ASCE)0733-9429(1995)121:6(453)

Nama, A.H., 2011. Estimating the sediment transport capacity of Tigris river within Al Mosul city. *Journal of Engineering*, 17(03), pp. 473–485. https://doi.org/10.31026/j.eng.2011.03.10.

Ohmoto, T., Hirakawa, R. and Koreeda, N., 2002. Effects of water surface oscillation on turbulent flow in an open channel with a series of spur dikes. *Hydraulic Measurements and Experimental Methods*, pp. 1–10. http://dx.doi.org/10.1061/40655(2002)108

Razzaq, H.K., Abed, B.Sh. and Al-Saadi, A.J.J., 2024. Simulation of bed change in Al-Musayyab Canal using HEC-RAS software. *Journal of Engineering*, 30(05), pp. 114–131. https://doi.org/10.31026/j.eng.2024.05.08

Shampa, Hasegawa, Y., Nakagawa, H., Takebayashi, H. and Kawaike, K., 2020. Three-dimensional flow characteristics in slit-type permeable spur dike fields: efficacy in riverbank protection. *Water*, 12(4), P. 964. https://doi.org/10.3390/w12040964

Sharma, K. and Mohapatra, P.K., 2012. Separation zone in flow past a spur dyke on rigid bed meandering channel. *Journal of Hydraulic Engineering*, 138(10), pp. 897–901. http://dx.doi.org/10.1061/(ASCE)HY.1943-7900.0000586

Siefken, S., Ettema, R., Posner, A., Baird, D., Holste, N., Dombroski, D.E. and Padilla, R.S., 2021. Optimal configuration of rock vanes and bendway weirs for river bends: Numerical-model insights. *Journal of Hydraulic Engineering*, 147(5), P. 04021013. https://doi.org/10.1061/(ASCE)HY.1943-7900.0001871

Uijttewaal, W.S., 2005. Effects of groyne layout on the flow in groyne fields: Laboratory experiments. *Journal of Hydraulic Engineering*, 131(9), pp. 782–791. https://doi.org/10.1061/(ASCE)0733-9429(2005)131:9(782)

Vaghefi, M., Ghodsian, M. and Akbari, M., 2017. Experimental investigation on 3D flow around a single T-shaped spur dike in a bend. *Periodica Polytechnica Civil Engineering*, 61(3), pp. 462–470. https://doi.org/10.3311/PPci.7999

مقارنة التأثير الهيدروليكي للسنون المستقيمة والمنحنية في قناة منحنية

يوسف زيد سالم*، حيدر عبد الامير خضير

قسم هندسة الموارد المائية، كلية الهندسة، جامعة بغداد، بغداد، العراق

الخلاصة

تعد ديناميكيات التدفق والاضطراب المحيط بالسنون في القناة المنحنية ظاهرة معقدة للغاية. تركز هذه الدراسة، التي تم أجرائها باستخدام برنامج هيك–راس الإصدار 6.5 على استخدام السنون المنحنية في القنوات المنحنية 180 درجة لغرض دراسة سلوك التدفق في الانحناء عن طريق حساب سرعة التدفق على طول الحافة الخارجية المقعرة، والتي يحدث فيها تآكل للجوانب عادة، وسرعة التدفق عند الحافة الداخلية، وحساب الدوامات التي تتشكل بين السنون. أظهرت النتائج أن السنون المنحنية تتفوق في الأداء على السنون المستقيمة الشائع استخدامها تحت تأثير نفس الظروف. أظهرت النتائج أن السنون المنحنية تفوقت على السنون المستقيمة المستخدمة في نفس الظروف. حيث ساهمت في خفض سرعة التدفق عند الحافة الخارجية بنسبة تصل إلى 99%، مقارنة بالسنون المستقيمة التي حققت انخفاضًا يتراوح بين 68% و98%. أما عند الحافة الداخلية، فقد أدى تقليل مقطع القناة إلى زيادة سرعة التدفق بنسبة 28% عند استخدام السنون المنحنية، و34% عند استخدام السنون المستقيمة. وبالإضافة إلى ذلك، سرعة الدوامات المتشكلة بين السنون المنحنية اقل مما هو عليه عند استخدام السنون المستقيمة مما يؤدي الى تقليل حدوث تآكل في أرضية القناة.

الكلمات المفتاحية: السنون، السنون المنحنية، السنون المستقيمة، القنوات المنحنية، هيك-راس